Fluid Inclusion Geochemistry as Guides to Separate Alteration Zones at Sungun Porphyry Copper Deposit

O. Asghari[iii]; A. Hezarkhani[ii]

ABSTRACT

The porphyry copper deposit (PCD) at Sungun is located in East Azarbaijan, NW of Iran. The Sungun porphyries occur as stocks and dikes ranging in composition from quartz monzodiorite through quartz monzonite and granodiorite to granite. The stocks are divided into two groups (1) Porphyry Stocks I and (2) Porphyry Stock II. Porphyry Stock II, hosting the copper ore, experienced intense hydro-fracturing leading to the formation of stockwork-type, veinlets and micro-veinlets of quartz, sulfides, carbonates, and sulfates. Three distinct types of hydrothermal alteration and sulfide mineralization are recognized at Sungun (1) hypogene, (2) contact metasomatic (skarn), and (3) supergene. Four types of hypogene alteration are developed at Sungun, potassic, propylitic, potassic–phyllic, and phyllic. Based upon their phase content, four types of fluid inclusions are common at Sungun (1) vapor, mono-phase (2) vapor-rich, two-phase, (3) liquid-rich two-phase, and (4) multi-phase. Halite is the principal solid phase. The distribution pattern, shape, and phase contents of fluid inclusions in quartz veinlets at Sungun are analogous to those from Bingham and Globe-Miami in western USA. We used multiphase inclusions to calculate the point pressure and hydrothermal fluid density. Four variables have been measured and calculated for forty seven separated samples, including the homogenization temperature, salinity, pressure and density.

Histograms of variables represented that no variable could separate potassic and phyllic alterations lonely. In potassic alteration zone, the average of homogenization temperature is 413.6 °C while in phyllic alteration, it is 375.9 °C. As it is expected in potassic alteration, the temperature of hydrothermal is higher than that in phyllic zone, but there is not high difference between them. The salinity of the hydrothermal has a high coherency with homogenization temperature, so the average amount of salinity in potassic samples is 46.3 (wt% NaCl) which is higher than phyllic samples. Based on the location of potassic alteration, it is expected that the lithostatic pressure is much more than the phyllic one, so it is realized that the average of pressure in the potassic alteration is ~1195 (bar) while the average pressure in phyllic is ~623 (bar). The amount of the density depends on the amount of the salinity of hydrothermal fluid, so the average density of the samples in potassic alteration is 1.124 (gr/cm^3) which is higher than that in phyllic zone (1.083 gr/cm^3).

KEYWORDS

Fluid Inclusion, Porphyry Copper Deposit, Sungun, Salinity, Homogenization Temperature.

1. INTRODUCTION

Porphyry Copper deposits generate where magmatic–hydrothermal fluids are expelled from crystallizing intermediate to granitic magmas in the plate tectonic convergence regions [1]. Cooling, depressurization, and reaction between the fluids and the wall rocks cause metals to precipitate in and around the fractures, forming veins with alteration envelopes. Fluid inclusion analyses indicate that they are trapped in porphyry Cu deposits and typically include halite-saturated brines and low-salinity vapor inclusions [2], [3], [4]. The formation of brine and vapor is inferred to result from a miscibility gap in the NaCl–H_2O system that coincides with the pressure (< 2200 bars) and temperature (300 to 600 °C) where most porphyry Cu deposits form [5], [6].

Fluid inclusion studies in porphyry copper deposits (PCDs) have proven to be an important tool for constraining the physico-chemical conditions of the

i. O. Asghari, Ph.D. student at Department of Mining and Metallurgy Engineering, Amirkabir University of Technology, Tehran, Iran (e-mail: o.asghari@aut.ac.ir).

ii. A. Hezarkhani is with the Department of Mining and Metallurgy Engineering, Amirkabir University of Technology, Tehran, Iran (e-mail: ardehez@aut.ac.ir).

hydrothermal fluids responsible for vast and pervasive alteration and mineralization processes. These fluid inclusion studies have shown many common features in such deposits throughout the world [7], [8], [9], [10], [11], [12], [13], [14].

At Sungun deposit, numerous cross-cutting quartz veinlets and micro-veinlets, developed in various stages of alteration and mineralization, provided suitable material for fluid inclusion investigations. Etminan was the first to recognize the presence of porphyry-type copper mineralization at Sungun through fluid inclusion studies [9]. Mehrpartou allocated a chapter of his Ph.D. thesis to fluid inclusion studies in subsurface samples [15]. Based upon systematic sub-surface sampling, more detailed studies of fluid inclusions were carried out by Calagari and comprehensive micro thermometric data were accumulated [16]. Additional fluid inclusion work on the Sungun PCD was presented by Hezarkhani and Williams-Jones [17], [18]. This research represents a more comprehensive fluid inclusion study of the Sungun PCD and provides substantial micro-thermometric data, furnishing a suitable basis for a new interpretation based on a powerful multivariate statistical method entitled discriminant analysis. This method consists of finding a transform which gives the maximum ratio of the difference between two group multivariate means to the multivariate variance within the two groups. It is closely related to multiple regression and trend-surface analysis. In the following research, by applying the discriminant analysis, six variables from the samples have been measured and calculated, and the result is used to separate the alteration zones (i.e., potassic and phyllic).

2. GEOLOGICAL SETTING

The Sungun PCD is located in about 100 km NE of Tabriz, in the NW part of Iran. The Sungun porphyries are of Oligo-Miocene age, and were intruded, as a sub-volcanic complex into Upper Cretaceous carbonate rocks, a series of Eocene arenaceous-argillaceous rocks, and a series of Oligocene dacitic breccias, tuffs and trachy-andesitic lavas [15], [16], [17], [18]. The Sungun porphyries occur as stocks and dikes, and are a series of calc-alkaline igneous rocks with a typical porphyritic texture. They are situated in the northwestern part of a NW–SE trending Cenozoic magmatic belt (Sahand-Bazman) within which the Sarcheshmeh PCD (Iran's largest one) is also located (see inset in Fig. 1). The Sungun stocks are divided into two groups: (1) Porphyry Stocks I and (2) Porphyry Stock II. The rock type in Porphyry Stocks I is typically quartz monzodiorite. Porphyry Stock II (which is investigated in this research) hosts the Sungun PCD and varies in composition from quartz monzonite through granodiorite to granite. Four series of cross-cutting dikes (DK1, DK2, DK3, DK4) varying in composition from quartz monzodiorite to granodiorite cut the Sungun stocks.

3. HYDROTHERMAL ALTERATION AND MINERALIZATION

Alteration and related mineralization in the Sungun porphyry copper deposit have been investigated by geological mapping, and detailed studies of the mineralogy, petrography and chemistry of a large number of drill cores and outcrop samples from various parts of the stock (Fig. 3). Hydrothermal alteration and mineralization at Sungun are centered on the stock II and were broadly synchronous with its emplacement. Early hydrothermal alteration was dominantly potassic and propylitic, and was followed by later Phyllic and argillic alteration.

A. Potassic alteration

The earliest alteration is represented by potassic mineral assemblages developed pervasively and as halos around veins in the deep and central parts of the Sungun stock [18]. Potassic alteration is characterized by K feldspar. This alteration displays a close spatial association with mineralization; perhaps as much as 60 percent of the copper and all the molybdenum were emplaced during this alteration episode. On average, potassically altered rocks contain 28 percent plagioclase, 33 percent orthoclase, 20 percent quartz, 15 percent ferromagnesian minerals (mainly biotite, and sericite and chlorite after biotite), and 4 percent chalcopyrite, pyrite, zircon, scheelite, uraninite, bismuthinite, and rutile [17] (Fig.3).

B. Transition alteration (potassic-phyllic)

Potassic alteration is overprinted by a large zone of pervasive transition alteration in the central part of the stock, which grades upwards into phyllic alteration. Transition alteration is characterized by albite replacement of more an-rich plagioclase, and albite rims on orthoclase. Minor sericite and pyrite also partially replaced plagioclase, biotite and hornblende. A distinguishing characteristic of this type of alteration is the white color of the affected rocks [17]. This change of color from the original gray to white reflects a strong depletion of ferromagnesian minerals like hornblende and biotite. In contrast to potassic alteration, K was depleted and Cu added, probably due to breakdown of K feldspar and addition of anhydrite, respectively. Other major elements were relatively unchanged. The most important change among trace elements was the depletion in Cu (Fig.2, 3).

C. Phyllic alteration

The change from transition alteration to phyllic alteration is gradual and is marked by an increase in the proportion of muscovite. Phyllic alteration is characterized by the replacement of almost all rock-forming silicates by sericite and quartz and overprints the earlier formed potassic and transition zones. Pyrite forms up to 5 vol. percent of the rock and occurs in veins and disseminations. Quartz veins are surrounded by weak

sericitic halos (Fig.2). Vein-hosted pyrite is partially replaced by chalcopyrite. Silicification was synchronous with phyllic alteration and variably affected much of the stock and most dikes. This observation is supported by whole-rock chemical analyses, which show that Si was added in higher proportion than for any other stage of the alteration [18]. In contrast to the transition zone, appreciable Cu was added to the rock during phyllic alteration. It is difficult to separate transition and phyllic alteration because of intense silicification during the latter alteration (Fig.3).

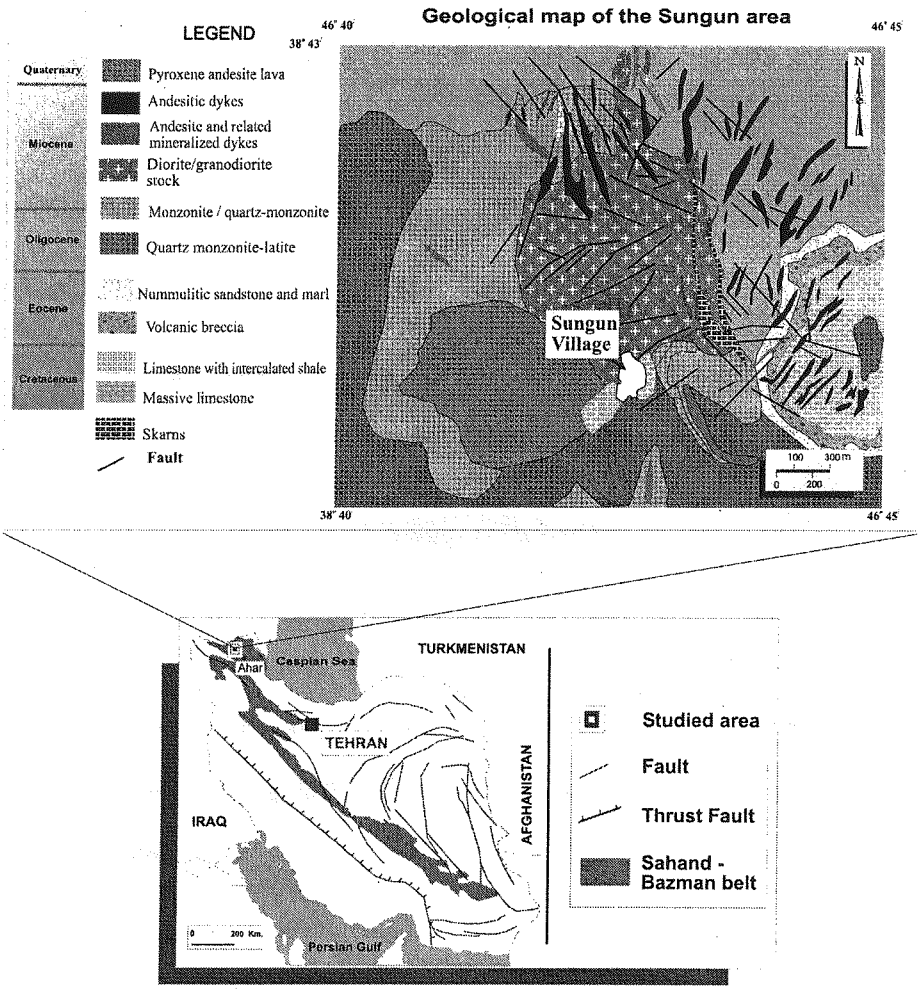

Fig. 1. Geological map of Iran showing Sahand-Bazman belt: Calc-alkaline volcanic and Quartz monzonite and quartz diorite intrusions of dominantly Miocene age, hosting Cu-Mo porphyry style mineralization and geological map of the Sungun deposit area, showing field relationships among the various subtypes of Sungun intrusive rocks, and the outline of the mineralized zone. The porphyritic quartz monzonite rims all other porphyritic plutons to the south and west, and Cretaceous limestone and associated skarn border the north and east. Andesite and andesitic dikes are distributed through the north and western parts of the deposit (mainly outside the stock). Mineralized dikes intrude the quartz monzonite stock in the central part of the deposit. Skarn-type alteration (and associated mineralization) occurs predominantly adjacent to the eastern margin of the stock [15], [18].

D. Argillic

Feldspar is locally altered to clay down to a depth of 400 m, and within 80 m of the erosional surface the entire rock has been altered to an assemblage of clay minerals, hematite and quartz. The affected rocks are soft and white colored. XRD analyses indicate that kaolinite is the dominant phyllosilicate, and that it is accompanied by illite. The shallow alteration is interpreted to represent a supergene blanket over the deposit and the deeper clay alteration of feldspar may have had the same origin. However, the possibility cannot be excluded that the latter represents an advanced argillic stage of the hypogene alteration.

E. Mineralization

Hypogene copper mineralization was introduced during potassic alteration and to a lesser extent, during phyllic alteration, and exists as disseminations and in veinlets form. During potassic alteration, the copper was deposited as chalcopyrite and minor bornite; later hypogene copper was deposited mainly as chalcopyrite. Hypogene molybdenite was concentrated mainly in the deep part of the stock and is associated exclusively with potassic

alteration, where it is found in quartz veins accompanied by K feldspar, anhydrite, sericite, and lesser chalcopyrite. The concentration of sulfides and copper mineralization increases outward from the central part of the stock, with the latter generally reaching a maximum of >0.8 wt percent along the interface between the potassic and phyllic alteration zones and in silicified phyllically altered rocks; sulfide concentrations, mainly pyrite, are highest in the phyllic alteration zone. The ratio of pyrite to chalcopyrite increases from 4:1 in the outer parts of the potassic alteration zone to 15:1 toward the margins of the stock.

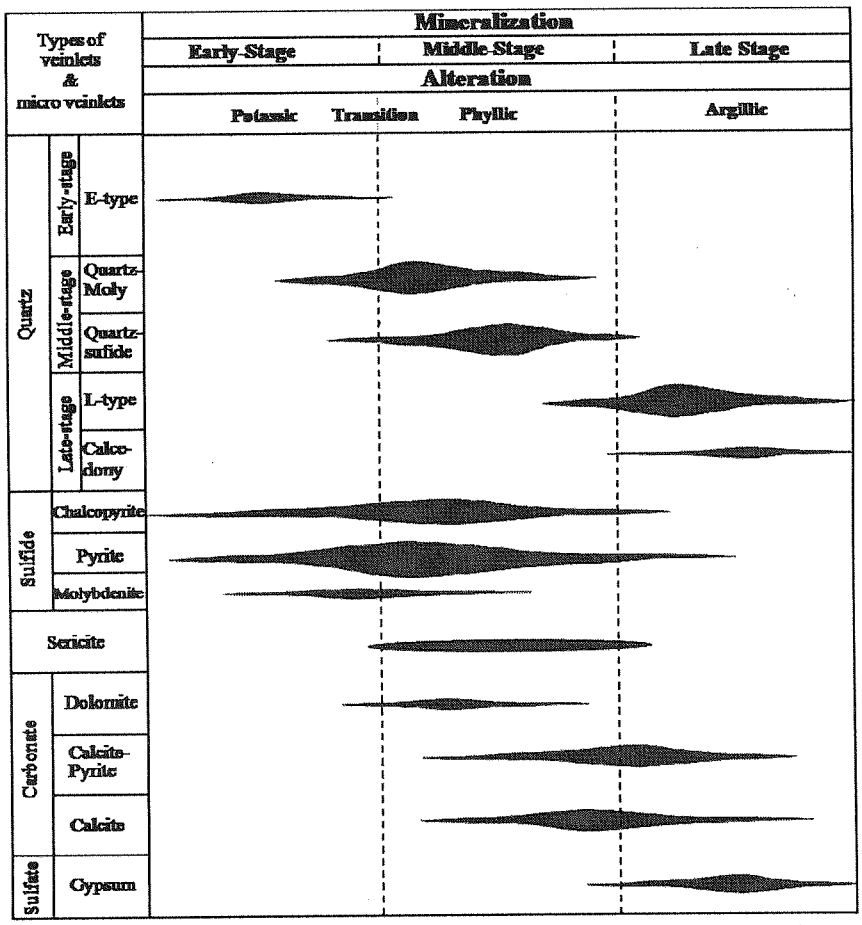

Fig. 2. Paragenetic sequence of the development of various types of veinlets and micro-veinlets in porphyry stock II at Sungun. The thickness of the horizontal bars is related to the relative abundance of the veinlets in the porphyry system [16].

4. FLUID INCLUSIONS

Fluid inclusions are abundant in quartz of all vein types, and range in diameter from 1μm up to 15 μm. The majority of inclusions examined during this study had diameters of 4-12 μm. Forty seven sub-surface samples containing quartz veinlets from diamond drill holes within the hypogene alteration zones in Porphyry Stock II were selected for thermometric analyses.

A. Method of investigation

The samples were initially prepared for microscopic examination. Based on mineral content, we found the origin of alteration and categorized them into potassic and phyllic (Table 3). The distribution pattern, shape size, and phase content of fluid inclusions within the quartz crystals were examined applying microscope (Table 1). Temperatures of phase changes in fluid inclusions were measured with a Fluid Inc. U.S.G.S.-type gas-flow (Linkam Operating System) stage, which operates by passing preheated or precooled N_2 gas around the sample. Stage calibration was performed using synthetic and/or well-known fluid inclusions. Accuracy at the standard reference temperatures was ±0.2°C at –56.6°C (triple point of CO_2), ±0.1°C at 0°C (melting point of ice), ±2°C at 374.1°C (critical homogenization of H_2O), and ±9°C at 573°C (alpha to beta quartz transition). The heating rate was approximately 1°C/min near the temperatures of phase transitions.

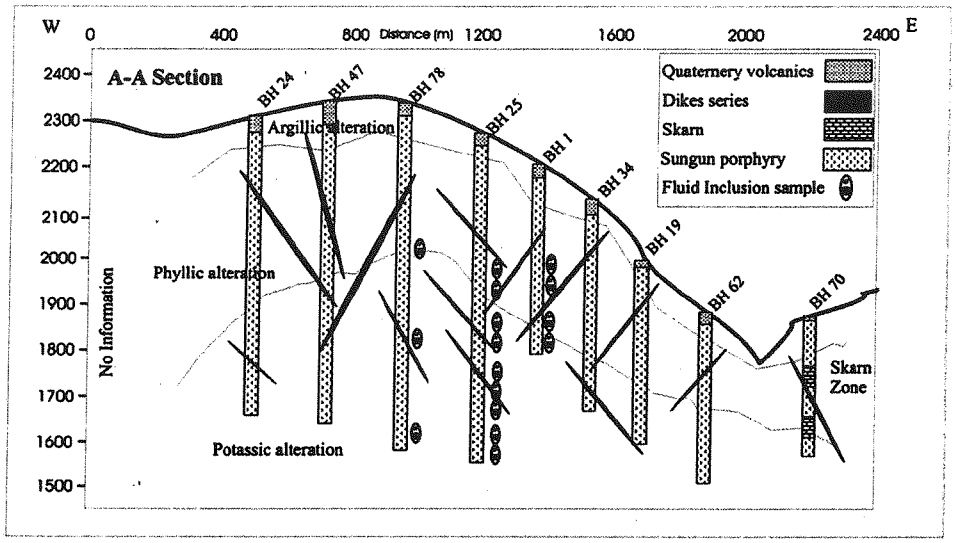

Fig. 3. Profile along A-A in Fig. 1 illustrating the position of diamond drill holes, dike series, and the pattern of hypogene alteration zones (potassic, phyllic and argillic) in Porphyry Stock II. (Asghari, 2006).

B. Fluid inclusion petrology

Quartz crystals exist within almost all types of quartz veinlets (late-type, quartz-sulfide, quartz-molybdenite and early type (Fig. 2). Fluid inclusions within the quartz crystals in quartz-sulfide and quartz-molybdenite veinlets were chosen for micro-thermometric analyses for two important reasons: (1) the inclusions are intimately associated with copper and molybdenum sulfides, (2) these veinlets contain inclusions >7 μm which allow for more confident thermometric analysis. Based upon their phase content, four types of inclusion, are present at Sungun: (1) mono-phase vapor, (2) vapor-rich 2-phase (3) liquid-rich 2-phase and (4) multi-phase solid. Halite crystals are larger than the other solids and can be readily distinguished by their cubic shape. Similar characteristics are seen in fluid inclusion assemblages from other PCDs such as El Salvador, Chile [20], Santa Rita, New Mexico [21], Bingham, Utah [22], Yandera and Panguna, Papua New Guinea [23], Bajo de la Alumbrera, Argentina [24].

C. Micro-thermometric analysis

Thermometric analyses were performed principally on fluid inclusions which were relatively large (>7 μm). Two common thermometric procedures, freezing and heating, were employed to determine the approximate salinity (wt% NaCl equivalent) and homogenization temperature (T_H), respectively (Table 1). The collected data were converted into corresponding salinity values by using diagrams for NaCl–H_2O system [25]. The heating stage was used for all types of inclusion (except for mono-phase vapor inclusions). For non-halite bearing inclusions the homogenization temperature of liquid and vapor (either L+V→L or L+V→V) was recorded. In the halite-bearing inclusions, two points: (1) $T_{s(NaCl)}$ (the temperature at which halite dissolves) and (2) $T_{H(L-V)}$ (temperature of vapor and liquid homogenization) were recorded.

D. Homogenization temperatures

The temperatures of initial (T_e) and final melting of ice ($T_{m\ ice}$) were measured on types LV, VL, and LVH fluid inclusions. The temperature of initial ice melting (Te) of most LV fluid inclusions was between –23° and –24.2°C, suggesting that NaCl is the principal salt in solution. The T_e value of VL fluid inclusions ranges from – 19.7° to – 46.1° C with a mode of ~–22°C, suggesting that Na and K are the dominant cations in the solution, but that there are significant concentrations of divalent cations. The eutectic temperatures that could be measured in LVH inclusions range from –29.9 to –64.2 °C, suggesting important concentrations of Fe, Mg, Ca, and/or other components in addition to Na and K in this type of inclusion. The $T_{m\ ice}$ values for LV inclusions range from –5.1° to –8.2°C (Table 4), corresponding to salinities of 5.7 wt% NaCl equiv., respectively [26]. The T_{mice} value for VL inclusions varies from –0.4°C to –12.1°C, which corresponds to a salinity of between 0.8 and 12.2 wt% NaCl equivalent.

Table 1: Descriptive statistics of raw data based on fluid inclusion study and micro thermometry for 845 measurements in 47 samples.

Statistical parameter	Salinity (%)	T_H (°C)	T_m (°C)	T_e (°C)	Size (μ^2)	L/V Ratio
Mean	23.98	355.10	-7.56	-37.90	22.34	2.87
Standard Deviation	18.66	92.66	5.51	11.75	10.43	2.66
Sample Variance	348.34	8585.82	30.34	138.03	108.79	7.06
Minimum	0.20	88.00	-33.00	-67.40	6.00	0.11
Maximum	65.45	620.00	-0.50	-4.00	70.00	19.00

LV fluid inclusions homogenize to liquid T_h (L+V→L) at temperatures between 523 and 298.1 °C. Most of VL inclusions homogenize to vapor T_h (V+L→V) between 351° and 600 (°C). The frequency distribution of halite-bearing inclusions homogenizing by halite disappearance

($T_{s(NaCl)} > T_{H(L-V)}$) display a wide range of $T_{s(NaCl)}$ values, varying from 220 to 583 (°C). Salinities based on the halite dissolution temperature range from 29.7 to 61.1 wt % NaCl equivalent [26]. The halite-bearing inclusions homogenizing by simultaneous disappearance of halite vapor and/or by vapor disappearance ($T_{s(NaCl)} \leq T_{H(L-V)}$) show a similar range of distribution and their $T_{H(L-V)}$ values vary from 200 to 580 (°C) (Table 3). Some LVH inclusions homogenized by vapor disappearance and by contrast, some LVH inclusions homogenized mainly by halite dissolution. Anhydrite and chalcopyrite did not dissolve on heating to temperatures in excess of 600°C.

E. Salinity in the inclusion fluids

Halite-bearing and non-halite-bearing liquid-rich inclusions at Sungun exhibit a wide variation in salinity, ranging from 0.2 to 65.5 wt% (Fig. 4).

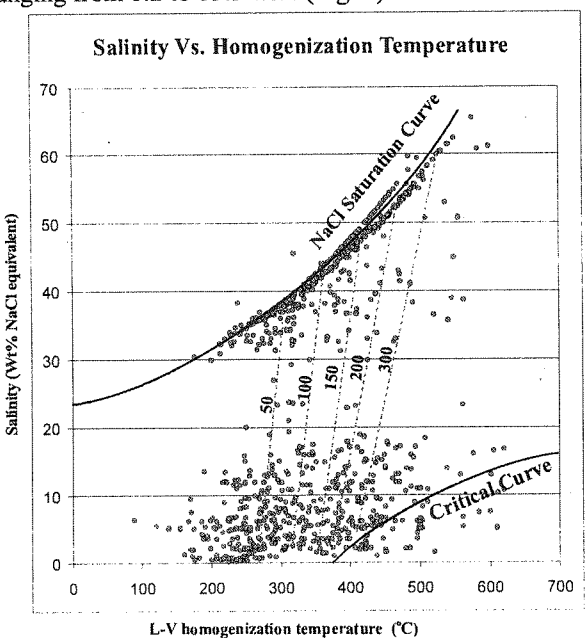

Fig. 4. Salinity versus TH(L-V) illustrating the distribution pattern of the data points relative to the NaCl saturation and critical curves (NaCl saturation and critical curves from Ahmad and Rose (1980). dashed lines referring to vapor pressures of NaCl solutions at the indicated temperatures and salinity from Roedder (1984)).

As shown by Fig. 6, it can sharply divide into 2 populations; low salinity (less than 27 wt% NaCl) and high salinity (between 27 wt% NaCl and 65.5 wt%). Scatter plot of salinity versus T_H (Fig. 6) shows there is high correlation coefficient factor between salinity and T_H in high saline inclusions ($r_{\text{correlation coefficient}} = 94\%$). But there is no correlation between low saline and T_H($r_{\text{correlation coefficient}} = 4\%$).

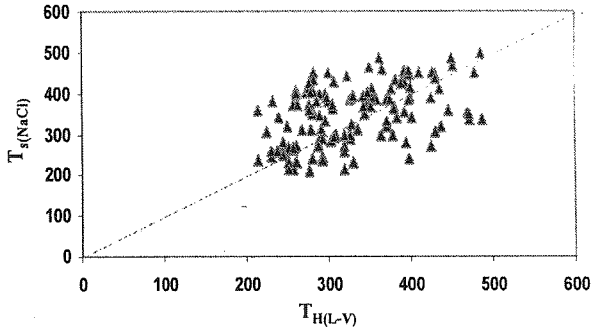

Fig. 5. Liquid-vapor homogenization temperature [TH(L-V)] versus halite dissolution temperature [TH(NaCl)] for halite - bearing inclusions at Sungun (the diagonal line [TH(L-V) = Ts(NaCl)]. For calculating the pressure we used points over the diagonal line, where Ts(NaCl) > TH(L-V) [25].

There are great many halite-bearing fluid inclusions which have $T_{s(NaCl)} > T_{H(L-V)}$ and the discrepancy between $T_{s(NaCl)}$ and $T_{H(L-V)}$ in some inclusions may reach >91 °C (Fig. 5). These inclusions may suggest entrapment of supersaturated (with respect to NaCl) fluid. However, there are still many halite-bearing inclusions whose data points lie around and below the halite saturation curve ($T_{s(NaCl)} < T_{H(L-V)}$) (Fig. 4) which, in turn, denotes trapping of saturated and undersaturated fluids, respectively.

5. COMPARING THE RESULTS IN TWO ALTERATIONS

As we know, changes in salinity in high salinity fluid inclusions and their homogenization temperature is very harmonic and the correlation coefficient is around 84 percent (R^2=0.6923). In low temperature fluid inclusions, the salinity and the homogenization temperature do not show any harmonic relationships. Based on the Brown and Lamb method, to measure the point pressure, the applied fluid inclusions must be halite- and gas-bearing with high salinity ones, which is why that these types of fluid inclusions are used from now on [27]. Table 2 shows the statistical properties of the fluid inclusions with the salinities more than 27 wt% equivalent.

The point pressure and density of hydrothermal fluid density in the NaCl-H_2O system is calculated for 47 samples with using 3 parameters including Th→Halite (°C), Th→Vapor (°C) and salinity (wt% NaCl), based on Brown and lamb equation by the Flincor software [27]. Fluid pressure varies from 261 to 2148 bars (Table 3)

Table 2: Descriptive statistics of raw data for high salinity inclusions (more than 27 wt% NaCl).

Statistical parameter	Salinity	T_h	T_m	T_e	Size	L/V Ratio
Mean	42.99	375.30	-11.57	-46.92	24.48	3.40
SD	7.57	81.63	6.35	9.08	12.42	2.07
Variance	57.33	6663.7	40.27	82.50	154.30	4.29
Minimum	29.30	176.20	-33.00	-67.40	8.00	0.25
Maximum	65.45	600.00	-1.20	-26.00	70.00	9.00

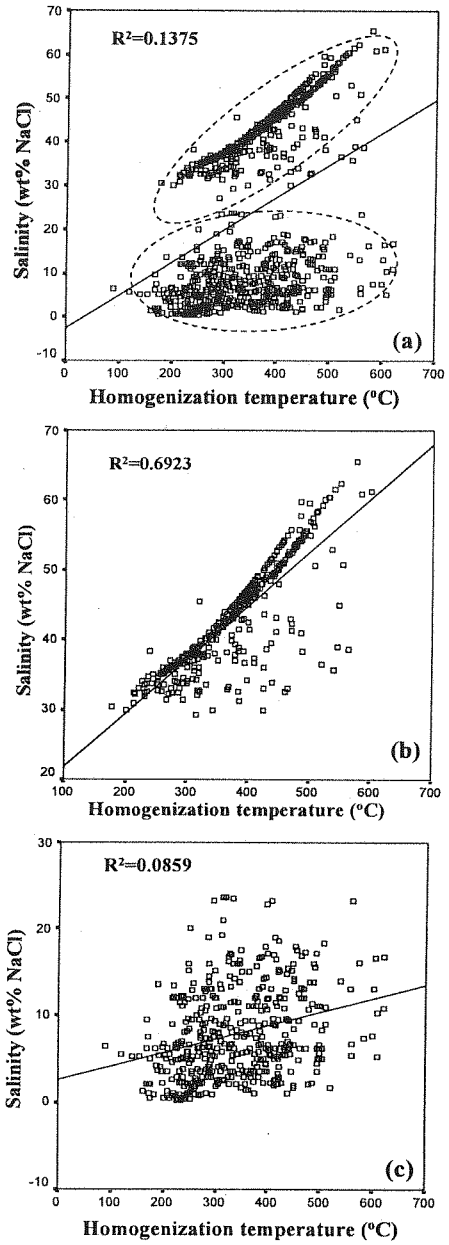

Figure 6. Scatter plot of salinity vs. homogenization temperature showing two different behaviors in salinity and Th. (a) a relatively high coherence between high salinities and Th (R^2=0.6923, coherent coefficient=0.83) and a low coherence between low salinities and Th (R^2=0.0859, coherent coefficient=0.29). □ shows the results of Th vs. Salinity.

The thirteen diamond drill holes within the Porphyry Stock II are drilled and 47 samples from drilled holes are collected. Approximately 200-400 gr. of each sample location from drilled cores were crushed and powdered for XRF analysis. The XRF analyses were carried out and accuracy and precision of the analytical procedure has been checked and the Cu grade of each sample achieved (Table 3). In potassic alteration the average of all parameters is higher than the phyllic one, but except the pressure, other variables have higher variety which is presented in variance (Table 4).

Table 3: Achieved data from 47 locations in 13 boreholes separated into potassic and phyllic. Based on microscopic studies 22 of them defined as potassic and 25 of them defined as phyllic alteration.

No	BH No.	Alt.	Th→H (°C)	salinity (%)	Th→V (°C)	pressure (bar)	density (gr/cm³)
1	BH 25	PHY	337	39.8	296.7	836	1.11
2	BH 25	PHY	351	42.5	319	770	1.149
3	BH 25	POT	393.8	46.5	368	711	1.12
4	BH 25	POT	371	44.8	349.7	583	1.11
5	BH 25	POT	372.7	45.1	320.5	1165	1.143
6	BH 25	POT	398	47.2	310.7	1981	1.194
7	BH 25	POT	357.9	43.1	277	1688	1.163
8	BH 25	POT	337	41.6	288	1030	1.137
9	BH 25	POT	347	42.6	320.7	619	1.115
10	BH 33	PHY	459.8	54.6	450.8	654	1.129
11	BH 106	POT	359.1	43.3	298	1406	1.189
12	BH 34	POT	397.5	45.5	300.4	2108	1.167
13	BH 1	PHY	410	46	395.0	560	1.077
14	BH 1	PHY	450	48	427	838	1.067
15	BH 1	PHY	430	47.8	410.5	713	1.082
16	BH 1	PHY	312	36	298	324	1.071
17	BH 1	PHY	234	33.5	212	446	1.128
18	BH 1	PHY	220	33	200	410	1.134
19	BH 1	PHY	250	34	225	502	1.121
20	BH 2	PHY	350	37	343	261	1.035
21	BH 2	PHY	355	38	344	334	1.044
22	BH 2	PHY	414	46.9	384	854	1.098
23	BH 2	PHY	410	48	400	485	1.095
24	BH 2	PHY	422.5	49	408	602	1.099
25	BH 2	PHY	380	36	349	655	1.019
26	BH 2	PHY	399	36	393	342	0.973
27	BH 2	PHY	428	46	414	590	1.057
28	BH 3	PHY	382	38.3	337	913	1.054
29	BH 3	PHY	425	46.4	406.5	664	1.069
30	BH 4	POT	356	42	331	599	1.098
31	BH 5	PHY	404	46	390	528	1.082
32	BH 6	POT	385	45.5	381	303	1.085
33	BH 78	POT	461	52.7	424.4	1257	1.13
34	BH 78	POT	431	47.7	398	965	1.093
35	BH 78	POT	444	49.9	403	1210	1.115
36	BH 84	POT	442.1	49.7	410	1020	1.105
37	BH 84	POT	454.7	51.1	403	1483	1.13
38	BH 86	PHY	404	45.4	388	557	1.077
39	BH 104	POT	418.3	47.25	355	1503	1.132
40	BH 104	POT	583	60.9	550	2148	1.134
41	BH 104	POT	474.5	53.6	432	1452	1.134
42	BH 104	POT	406	46.65	362	1098	1.118
43	BH 106	PHY	393.7	45.15	358	875	1.105
44	BH 106	PHY	389	44.54	335	1214	1.122
45	BH 106	PHY	387.6	43.8	363	646	1.085
46	BH 106	POT	462	32.6	408	998	1.136
47	BH 106	POT	447	38.48	404	962	0.987

Table 4: Descriptive statistics of 25 samples from phyllic alteration and 22 samples from potassic alteration.

	Desc.	Th→H	Salinity	Th→V	Pressure	Density
Potassic	Mean	413.6	46.3	367.9	1195	1.1243
	S.D.	56.4	5.7	62.6	498	0.0415
	Var.	3181.5	32.7	3924.6	247652	0.0017
	Min	337.0	32.6	277.0	303	0.9870
	Max	583.0	60.9	550.0	2148	1.1940
Phyllic	Mean	375.9	42.5	3539	623	1.0833
	S.D.	63.6	5.8	66.1	222	0.0398
	Var.	4039.1	34.0	4374	49497	0.0018
	Min	220.0	33.0	200.0	261	0.9730
	Max	459.8	54.6	450.8	1214	1.1490
Total	Mean	393.54	44.24	360.44	890.68	1.10

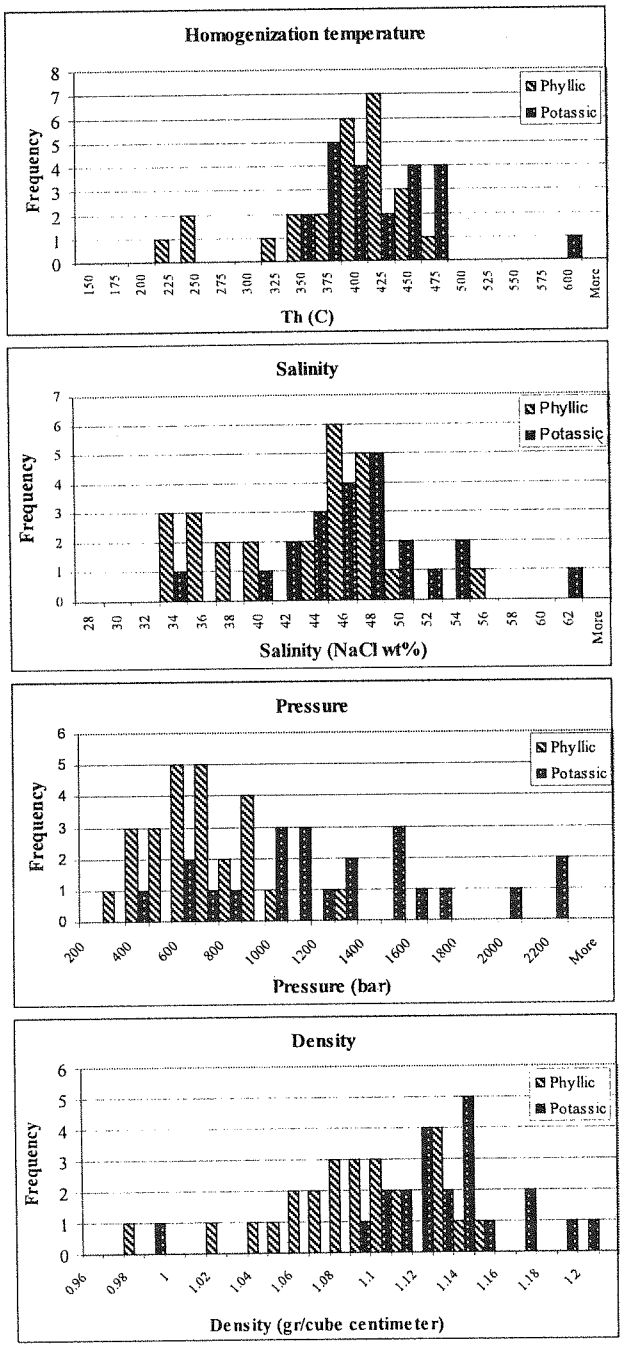

Fig. 7. Histograms of Homogenization temperature, salinity, pressure and density for 47 analyzed and calculated points based on F.I. data shows, there is not a sharp boundary between two potassic and phyllic alterations and they are like two mixed populations.

6. SUMMARY AND CONCLUSIONS

Early hydrothermal alteration produced a potassic assemblage (orthoclase-biotite) in the central part of the Sungun stock, propylitic alteration occurred contemporaneously with potassic alteration. But in the peripheral parts of the stock, and phyllic alteration occurred later, overprinting these earlier alterations. Based on fluid inclusion studies in the Sungun deposit, potassic alteration and associated Cu mineralization were caused by a high temperature and high salinity fluid of dominantly magmatic origin. The early hydrothermal fluids are represented by high temperature (340 °C to 500 °C), high salinity (up to 60 wt % NaCl equiv.) liquid-rich fluid inclusions, and high temperature (320 °C to 550 °C), low-salinity, vapor-rich inclusions. Phyllic alteration and copper leaching resulted from the inflow of oxidized and acidic meteoric waters with decreasing temperature (ranging from 300-380 °C, with a mode of 360 °C) of the system.

Histograms of variables from forty seven samples presented that no variable could separate potassic and phyllic alterations lonely. Results are as follows:

- In potassic alteration, the average of homogenization temperature is 413.6 °C while in phyllic alteration it is 375.9 °C. As it is expected in potassic alteration, the temperature of hydrothermal is higher than the phyllic one, but there is not much difference between them.
- The salinity of the hydrothermal has a high coherency with homogenization temperature, so the average amount of salinity in potassic samples is 46.3 (wt% NaCl) which is higher than phyllic samples
- Based on the location of potassic alteration, which is located beneath the phyllic alteration (Lowell and Guilbert model), we expect the lithostatic pressure is much more than the phyllic one, so it is realized that the average of pressure in the potassic alteration is 1195 (bar) while the pressure average in phyllic is 623 (bar) [28].
- The amount of the density depends on the amount of the salinity of hydrothermal fluid, so the average density of the samples in potassic alteration is 1.124 (gr/cm^3) which is higher than the phyllic one (1.083 gr/cm^3).

7. REFERENCES

[1] Burnham, C. W., 1979, Magmas and hydrothermal fluids: in Geochemistry of hydrothermal ore deposits, H. L. Barnes, John Wiley & Sons, Inc., p. 71- 136.

[2] Roedder, E., 1971. Fluid inclusion studies on the porphyry copper-type ore deposits at Bingham (Utah), Butte (Montana), and Climax (Colorado), Economic Geology, 66, 98–120.

[3] Roedder, E., 1984. Fluid inclusions, Reviews in Mineralogy, vol. 12. Book Crafters, Inc, Michigan, p. 644.

[4] Beane, R.E., Bodnar, R.J., 1995. Hydrothermal fluids and hydrothermal alteration in porphyry copper deposits. In: Wahl, P.W., Bolm, J.G. (Eds.), Porphyry Copper Deposits of the American Cordillera, Tucson, Arizona, Arizona Geological Society, Arizona, pp. 83–93.

[5] Sourirajan, S., Kennedy, G.C., 1962. The system H_2O–NaCl at elevated temperatures and pressures. American Journal of Science 260, 115–141.

[6] Urusova, M.A., 1975. Volume properties of aqueous solutions of sodium chloride at elevated temperatures and pressures. Russian Journal of Inorganic Chemistry 20, 1717–1721.

[7] Nash, J.T., Theodore, T.G., 1971. Ore fluids in the porphyry copper deposit at Copper Canyon, Nevada. Economic Geology 66, 385–399.

[8] Nash, J.T., 1976. Fluid inclusion petrology, data from porphyry copper deposits and applications to exploration. United States Geological Survey, Professional Paper, 907-D, p. 16

[9] Etminan, H., 1977. The discovery of porphyry copper–molybdenum mineralization adjacent to Sungun village in the

northwest of Ahar and a proposed program for its detailed exploration. Confidential Report, Geological Report, Geological Survey of Iran, p. 26
[10] Chivas, A.R., Wilkins, W.T., 1977. Fluid inclusion studies in relation to hydrothermal alteration and mineralization at the Koloula porphyry copper prospect, Guadalcanal. Economic Geology 72, 153–169.
[11] Eastoe, C.J., 1978. A fluid inclusion study of the Panguna porphyry copper deposit Bougainville, Papua New Guinea. Economic Geology 73, 721–748.
[12] Beane, R.E., Titley, S.R., 1981. Porphyry copper deposits, alteration and mineralization, part II. Economic Geology 75, 235–269.
[13] Reynolds, T.J., Beane, R.E., 1985. Evolution of hydrothermal fluid characteristics at the Santa Rita, New Mexico, porphyry copper deposit. Economic Geology 80, 1328–1347.
[14] Quan, R.A., Cloke, P.L., Kesler, S.E., 1987. Chemical analyses of halite trend inclusions from the Granisle porphyry copper deposit, British Columbia. Economic Geology 82, 1912–1930.
[15] Mehrpartou, M., 1993. Contributions to the geology, geochemistry, ore genesis and fluid inclusion investigations on Sungun Cu-Mo porphyry deposit, northwest of Iran. Unpublished PhD Thesis. University of Hamburg, Germany, p. 245
[16] Calagarj A.A., Pattrick, R.A.D., Polya, D.A., 2001. Veinlets and microveinlets studies in Sungun porphyry copper deposit, East Azarbaidjan, Iran. Quarterly Journal of Geosciences 10 (39/40), 70–79.Geological Survey of Iran.
[17] Hezarkhani, A., (2006), Petrology of intrusive rocks within the Sungun Porphyry Copper Deposit, Azarbaijan, Iran. Journal of Asian Earth Sciences. V. 73, P. 326-340.
[18] Hezarkhani, A., Williams-Jones, A.E., 1998. Controls of alteration and mineralization in the Sungun porphyry copper deposit, Iran: Evidence from fluid inclusions and stable isotopes. Economic Geology 93, 651–670.
[19] Emami, M.H., Babakhani, A.R., 1991. Studies of geology, petrology, and litho-geochemistry of Sungun Cu–Mo deposit, Iranian Ministry of Mines and Metals, p. 61.
[20] Gustafson, L.B., Hunt, J.P., 1975. The porphyry copper deposit at El Salvador, Chile. Economic Geology 70, 875–912.
[21] Ahmad, S.N., Rose, A.W., 1980. Fluid inclusions in porphyry and skarn ore at Santa Rita, New Mexico. Economic Geology 75, 229–250.
[22] Roedder, E., Bodnar, R.J., 1980. Geologic pressure determination from fluid inclusion studies. Annual Review of Earth and Planetary Science 8, 263–301.
[23] Watmuff, G., 1978. Geology and alteration-mineralization zoning in the central portion of the Yandera porphyry copper prospect, Papua New Guinea. Economic Geology 73, 829–856.
[24] Ulrich, T., Gunther, D., Heinrich, C.A., 2001. The evolution of a porphyry Cu–Au deposit, based on LA-ICP-MS analysis of fluid inclusions, Bajo de la Alumbrera, Argentina. Economic Geology 96, 1743–1774.
[25] Shepherd, T., Rankin, A.H., Alderton, D.H.M., 1985. A Practical Guide to Fluid Inclusion Studies, Blackie, London, p. 239.
[26] Sterner, S. M., Hall, D. L., and Bodnar, R. J., 1988, Synthetic fluid inclusions. V. Solubility of the system NaCl-KCl-H_2O under vapour-saturated conditions. Geochemica et Cosmochimica Acta, V. 52, p. 989-1005.
[27] Brown, P. E., 1989, FLINCOR: a microcomputer program for the reduction and investigation of fluid inclusion data. Am. Mineral. 74, 1390–1393.
[28] Lowell, J. D., and Guilbert, J. M., 1970, Lateral and vertical alteration-mineralization zoning in porphyry ore deposits. Economic geology: v. 65, p. 373-408.